2018 RISP International Workshop on Nonlinear Circuits,
Communications and Signal Processing (NCSP2018)
Honolulu, Hawaii, USA, March 4-7, 2018

Effect of Changing Coupling Strength to Synchronization Phenomena in Coupled van der Pol Oscillators

Vu Minh Hien, Minh Hai Tran, Yoko Uwate and Yoshifumi Nishio

†Dept. of Electrical and Electronic Engineering, Tokushima University,
2-1 Minamijosanjima, Tokushima, 770-8506 Japan
Email: {hien, minhhai, uwate, nishio}@ee.tokushima-u.ac.jp

Abstract

In this study, synchronization phenomena in coupled oscillators containing star structure connected to another oscillator is investigated. We focus on the phase difference between two oscillators when coupling strength is changed. Furthermore, we also investigate the effect of the initial condition. By using computer simulations, we observe synchronization phenomena of the system and apply theoretical analysis to confirm computer simulation results.

1. Introduction

Synchronization phenomena can be observed everywhere in our world, such as in firefly luminescence, birds and frogs crying, human aplause and so on. Synchronization phenomena in coupled van der Pol oscillators are good models to describe various higher-dimensional nonlinear phenomena in the field of natural science. Synchronization phenomena has a long history of researches and they have been reported in many researches of engineering fields [1] - [2]. Furthermore, the applications of synchronization phenomena have been also found in chemical, physical and biological fields [3] - [4]. Therefore, investigation of synchronization phenomena observed in coupled oscillatory systems is an important issue. However, there are not many discussions about coupled complex oscillatory networks by using electrical oscillators.

The van der Pol oscillator is a simple circuit as shown in Fig. 1. It consists of an inductor, a capacitor and a nonlinear resistor.

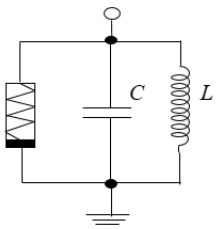

Figure 1: van der Pol oscillator.

In this study, we propose a new type of coupled van der Pol oscillators: Star structure connected to another oscillator. By carring out computer simulations and theoretical analysis, the relationship of the model between synchronization phenomena and coupling strength is investigated.

2. Circuit Model

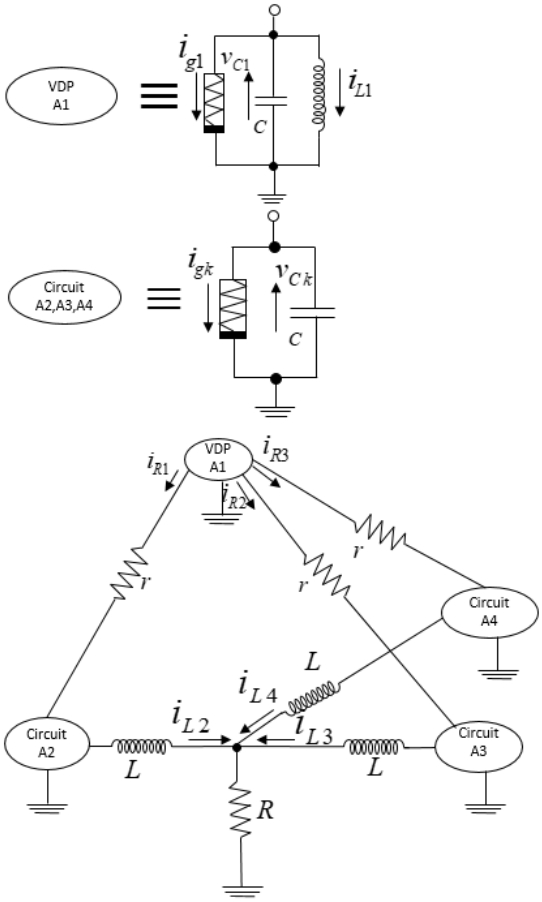

Figure 2: Circuit model.

The proposed circuit is shown in Fig. 2. We use three van der Pol oscillators coupled as star structure that connected to another oscillator via resistors r. We investigate synchronization phenomena by changing coupling strength of the resistors.

With v_{C1} v_{C2}, v_{C3}, and v_{C4} denote capacitor's voltage and i_{L1} i_{L2}, i_{L3}, and i_{L4} denote inductor's electric current.

The circuit equations of VDP-A1 are given as folows:

$$\begin{aligned} C\frac{dv_{C1}}{dt} &= -i_{g1} - i_{L1} - i_{R1} - i_{R2} - i_{R3}, \\ L\frac{di_{L1}}{dt} &= v_1. \end{aligned} \tag{1}$$

The circuit equations of Circuit-A2, Circuit-A3, Circuit-A4 are given as follows:

$$\begin{aligned} C\frac{dv_{Ck}}{dt} &= -i_{gk} - i_{Lk} + i_{Rk}, \\ L\frac{di_{Lk}}{dt} &= v_k - R\sum_{m=2}^{4} i_{Lm}. \end{aligned} \tag{2}$$

where:

$$i_{Rk} = \frac{v_1 - v_k}{r},$$
$$(k = 2, 3, 4).$$

The characteristics of the nonlinear resistors are defined as follows:

$$i_{gk} = -g_1 v_k + g_3 v_k^3. \tag{3}$$

By changing the variables and parameters:

$$\begin{aligned} t &= \sqrt{LC}\tau, v_k = \sqrt{\frac{g_1}{3g_3}}x_k, \\ i_{Lk} &= \sqrt{\frac{g_1 C}{3g_3 L}}y_k, \alpha = g_1\sqrt{\frac{L}{C}}, \\ \beta &= \frac{1}{r}\sqrt{\frac{L}{C}}, \gamma = R\sqrt{\frac{C}{L}}, \\ &(k = 1, 2, 3, 4). \end{aligned} \tag{4}$$

the normalized circuit equations of VDP-A1 are given as follows:

$$\begin{cases} \dfrac{dx_1}{d\tau} = \alpha\left(x_1 - \dfrac{1}{3}x_1^3\right) - y_1 + \beta\left(3x_1 - \displaystyle\sum_{m=2}^{4} x_m\right) \\ \dfrac{dy_1}{d\tau} = x_1. \end{cases} \tag{5}$$

the normalized circuit equations of Circuit-A2, Circuit-A3, Circuit-A4 are given as follows:

$$\begin{cases} \dfrac{dx_k}{d\tau} = \alpha\left(x_k - \dfrac{1}{3}x_k^3\right) - y_k - \beta(x_1 - x_k) \\ \dfrac{dy_k}{d\tau} = x_k - \gamma\displaystyle\sum_{m=2}^{4} y_m, \end{cases} \tag{6}$$

$$(k = 2, 3, 4).$$

where parameters α, β, and the γ denote nonlinearity, the resistors r, and the resistor R, respectively.

3. Simulation Results

For the computer simulations, we calculates Eqs. (2)-(5) by using the Runge-Kutta method with the step size $h = 0.05$. We show the simulation results when the parameters of the circuit model are fixed as $\alpha = 0.01$, $\beta = 0.01$ and $\gamma = 0.006$.

Figure 3 shows the attractor of each oscillator with the horizontal axis is the voltage and the vertical axis is the electric current of each oscillator.

First, we investigate the effect of different the initial condition. As simulation results are shown in Fig. 4, we obtain that, by changing initial values, 2 oscillators of Circuit-A2, Circuit-A3, Circuit-A4 can become in-phase.

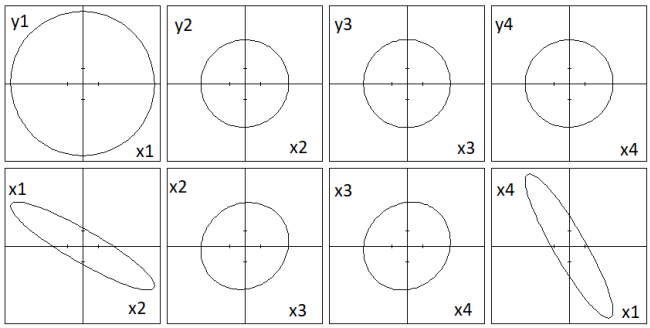

Figure 3: Attractor between adjacent oscillators ($\alpha = 0.01$, $\beta = 0.01$, $\gamma = 0.006$).

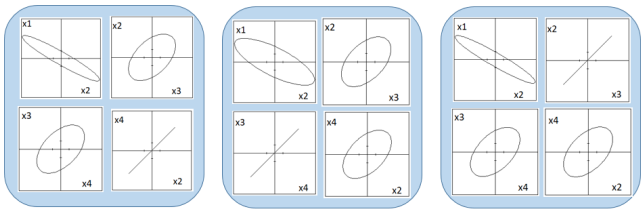

Figure 4: Phase difference ($\alpha = 0.01$, $\beta = 0.01$, $\gamma = 0.006$).

Next, we decrease the values of parameter γ from 0.006 to 0.005 and continue conducting computer simulation. In this case, all four oscillatos become synchronization with second, third and fourth oscillator (Circuit-A2, Circuit-A3, Circuit-A4) are in-phase and only first oscillator of VDP-A1 is anti-phase. The result of simulation is shown in Fig. 5.

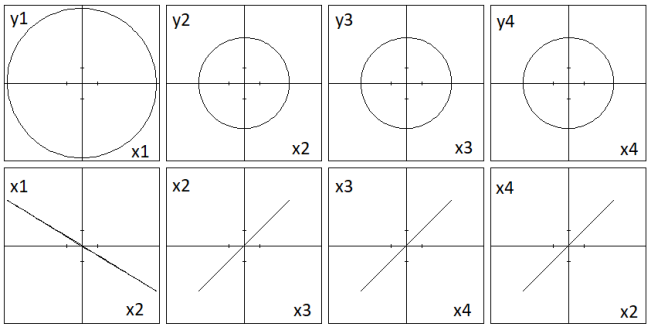

Figure 5: Phase difference ($\alpha = 0.01$, $\beta = 0.01$, $\gamma = 0.005$).

Figure 6, figure 7 and figure 8 show the computer simulation results of the phase difference when parameter γ is changed from 0.001 to 0.009, α is changed from 0.001 to 0.01 and β is changed from 0.007 to 0.016 with step size 0.001. In this case, we can obtain that, when value of parameter γ is smaller than 0.005, α is smaller than 0.006 and β is lager than 0.011, second, third, fourth oscillator are in-phase and only first oscillator VDP-A1 is anti-phase.

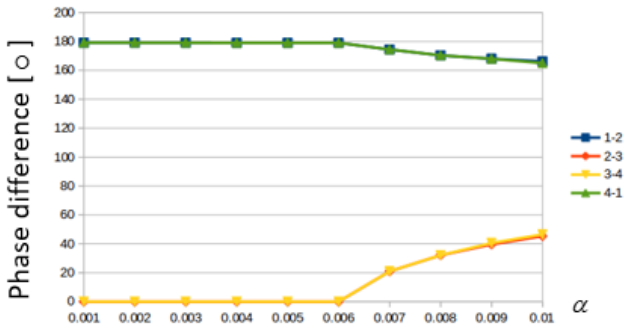

Figure 6: Phase difference ($\beta = 0.01$, $\gamma = 0.006$).

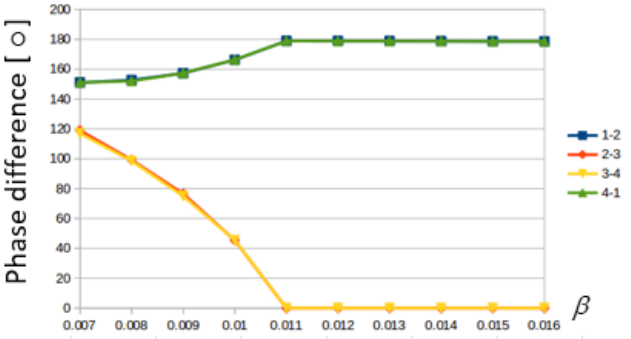

Figure 7: Phase difference ($\alpha = 0.01$, $\gamma = 0.006$).

Therefore, we can control synchronization phenomena by changing initial values or the coupling strengths.

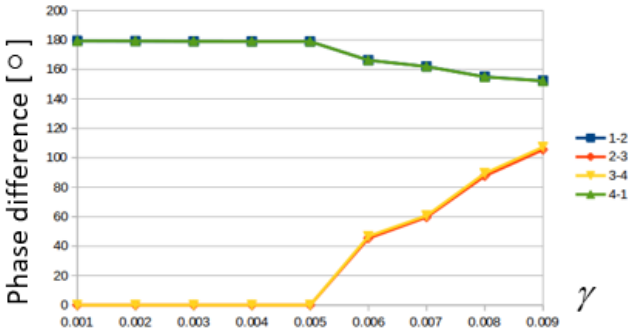

Figure 8: Phase difference ($\alpha = 0.01$, $\beta = 0.01$).

4. Theoretical Analysis

In this section, we apply theoretical analysis to comfirm above computer simulation results by using averaging method for Eqs. (5) and (6). We assume that $x_{1,k}$, $y_{1,k}$ can be considerd as below:

$$\begin{aligned} x_{1,k}(\tau) &= \rho_{1,k}(\tau)\cos(\tau + \theta_{1,k}(\tau)) \\ y_{1,k}(\tau) &= \rho_{1,k}(\tau)\sin(\tau + \theta_{1,k}(\tau)). \end{aligned} \tag{7}$$

Assign Eqs. (5)-(6) to Eqs. (7), we obtain:
VDP-A1:

$$\begin{aligned} \dot{\rho_1} &= \alpha(x_1 - \tfrac{1}{3}x_1^3)\cos\phi_1 - y_1\cos\phi_1 \\ &\quad +\beta(3x_1 - \sum_{n=2}^{4} x_n)\cos\phi_1 + x_1\sin\phi_1 \equiv X_1 \\ \dot{\theta_1} &= \frac{x_1\cos\phi_1}{\rho_1} - \frac{\alpha(x_1 - \frac{1}{3}x_1^3)\sin\phi_1}{\rho_1} + \frac{y_1\sin\phi_1}{\rho_1} \\ &\quad -\frac{\beta(3x_1 - \sum_{n=2}^{4} x_n)\sin\phi_1}{\rho_1} - 1 \equiv Y_1. \end{aligned} \tag{8}$$

Circuit-A2, Circuit-A3, Circuit-A4:

$$\begin{aligned} \dot{\rho_k} &= \alpha(x_k - \tfrac{1}{3}x_k^3)\cos\phi_k - y_k\cos\phi_k \\ &\quad -\beta(x_1 - x_k)\cos\phi_k + x_k\cos\phi_k \\ &\quad -\gamma\sum_{n=2}^{4} y_n\sin\phi_k \equiv X_k \\ \dot{\theta_k} &= \frac{x_k\cos\phi_k}{\rho_k} - \frac{\alpha(x_k - \frac{1}{3}x_k^3)\sin\phi_k}{\rho_k} + \frac{y_k\sin\phi_k}{\rho_k} \\ &\quad -\frac{\gamma\sum_{n=2}^{4} y_n\cos\phi_k}{\rho_k} - 1 \equiv Y_k, \end{aligned} \tag{9}$$

where

$$\phi_k = \tau + \theta_k$$
$$(k = 2, 3, 4)\ .$$

By averaging Eqs. (8)-(9) over on period, as averaging method's theory, $\rho_{1,k}$ and $\theta_{1,k}$ can be considered as constant and the values of $\dot{\rho_1}$,$\dot{\theta_1}$ can be calculated as:

VDP-A1:

$$\begin{aligned}\dot{\rho_1} &= \lim_{T\to\infty} \int_0^T X_1 d\tau \\ \dot{\theta_1} &= \lim_{T\to\infty} \int_0^T Y_1 d\tau.\end{aligned} \tag{10}$$

Circuit-A2, Circuit-A3, Circuit-A4:

$$\begin{aligned}\dot{\rho_k} &= \lim_{T\to\infty} \int_0^T X_k d\tau \\ \dot{\theta_k} &= \lim_{T\to\infty} \int_0^T Y_k d\tau.\end{aligned} \tag{11}$$

By solving the above equations, Eqs. (12) and (13) are obtained:

VDP-A1:

$$\begin{aligned}\dot{\rho_1} &= \frac{1}{2}\alpha\rho_1 - \frac{1}{8}\alpha{\rho_1}^3 + \beta\frac{3}{2}\rho_1 \\ &- \sum_{n=2}^{4}\frac{1}{2}\beta\rho_n\cos(\theta_n - \theta_1) \\ \dot{\theta_1} &= \frac{1}{2}\sum_{n=2}^{4}\frac{\rho_n}{\rho_1}\sin(\theta_n - \theta_1).\end{aligned} \tag{12}$$

Circuit-A2, Circuit-A3, Circuit-A4:

$$\begin{aligned}\dot{\rho_k} &= \frac{1}{2}\alpha\rho_k - \frac{1}{8}\alpha{\rho_k}^3 - \frac{1}{2}\beta\rho_1\cos(\theta_1 - \theta_k) \\ &+\frac{1}{2}\beta\rho_k - \sum_{n=2}^{4}\frac{1}{2}\gamma\rho_n\cos(\theta_n - \theta_k) \\ \dot{\theta_k} &= \frac{1}{2}\sum_{n=2}^{4}\frac{\rho_n}{\rho_k}\sin(\theta_k - \theta_n).\end{aligned} \tag{13}$$

In the steady state,

$\dot{\rho_{1,k}} = 0$ and $\dot{\theta_{1,k}} = 0$ must be satisfield. By solving Eqs. (12)-(13) we obtain:

$\frac{\rho_k}{\rho_1}$ as solution of below equation:

$$\frac{3}{2}\beta a^4 + \left(\frac{1}{2}\alpha + \frac{3}{2}\beta\right)a^3 - \left(\frac{1}{2}\alpha + \frac{1}{2}\beta - \frac{3}{2}\gamma\right)a - \frac{1}{2}\beta = 0. \tag{14}$$

For the phase difference:

$$\theta_1 - \theta_k = \pi$$

$$\theta_2 - \theta_3 = \theta_3 - \theta_4 = \theta_4 - \theta_2 = 0.$$

These theoretical rersults correspond with the computer simulation results. Table 1 summarizes the comparison between theoretical and simulation results when the parameters α, β are set as $\alpha = 0.01$, $\beta = 0.01$ and parameter γ is changed from 0.001 to 0.003. By solving Eq. (14), we can see that they match very well from below table.

Table 1: Comparison between theoretical and simulation results ($\alpha = 0.01$, $\beta = 0.01$).

	ρ_k/ρ_1	
γ	Theory	Simulation
0.001	0.711499	0.711512
0.002	0.686578	0.686588
0.003	0.660892	0.660902

5. Conclusions

In this study, we have investigated the synchronization phenomena in coupled oscillators containing star structure connected to another oscillator. By computer simulation, we have observed the synchronization phenomena by changing initial values and coupling strength. In the case of changing initial values, in three oscillators of Circuit-A2, Circuit-A3, Circuit-A4, two oscillators can become in-phase. By chaning coupling strength, all four oscillators can become synchronization with oscillators of Circuit-A2, Circuit-A3, Circuit-A4 are in-phase and only oscillator VDP-A1 is anti-phase. We also apply theoretical analysis to confirm these computer simulation results.

In the future, we experiment the proposed circuit model.

References

[1] K. Ueta, Y. Uwate and Y. Nishio, "Synchronization Phenomena in Complex Networks of van der Pol Oscillators", Proc. of NCSP'17, pp. 285-288, Mar. 2017.

[2] Y. Uwate, Y. Nishio and R. Stoop, "Synchronization in Three Coupled van der Pol Oscillators with Different Coupling Strength", Proc. of NCSP'10, pp. 109-112, Mar. 2010.

[3] F. Jhou, "Multistate and Multistage Synchronization of Hindmarsh-rose Neurons with Excitatory Chemical and Electrical Synapses", Proc. of IEEE, pp. 1335-1347, Jan. 2012.

[4] W. Wessel, "Synchronization and Coupling Analysis: Applied Cardiovascular Physics in Sleep Medicine", Proc. of EMBC'13, pp. 6567-6570, Jul. 2013.